ChemComm

COMMUNICATION

View Article Online
View Journal | View Issue



Cite this: *Chem. Commun.*, 2023, 59, 3134

Received 17th December 2022,
Accepted 15th February 2023

DOI: 10.1039/d2cc06881h

rsc.li/chemcomm



# Dynameric G-quadruplex–dextran hydrogels for cell growth applications†

Monica-Cornelia Sardaru,[a] Simona Morariu,[b] Oana-Elena Carp,[a] Elena-Laura Ursu,[a] Alexandru Rotaru *[a] and Mihail Barboiu *[c]

**Hybrid dextran–G-quartet produces tunable biocompatible three-dimensional thixotropic hydrogels, able to support cell growth.**

Supramolecular hydrogels assembled from low-molecular weight building block gelators are increasingly attractive for biomedical applications such as drug delivery or 3D cell culture.[1–4] In particular guanosine, a nucleoside and its analogues able to self-assemble into guanosine-quartets (G4) in the presence of various cations or into linear ribbons, have been extensively exploited for the fabrication of supramolecular gels.[4–8] The internal G4 network formed *via* H-bonding and metal coordination may be cross-linked *via* dynamic covalent bonds allowing for the encapsulation of large amounts of water molecules. It offers the entire hydrogel self-healable and injectable properties.[9–14] However, low-molecular weight-based hydrogels, including G4 ones, lack tunable strength and toughness and are difficult to handle, thus limiting their applications to some extent.[15] We recently reported reinforcement of G4-based hydrogels by dispersing single-walled carbon nanotubes as scaffolding pillars for the G4 matrix.[16] The guanosine nucleoside reacted with benzene-1,4-diboronic acid to form anionic diesters able to self-assemble into a G4 extensive network in the presence of $K^+$. The hydrophobic nature of guanosine in the network permitted stabilization of individual carbon nanotubes, thus considerably improving the hydrogel porosity and the amount of entrapped water molecules by the hydrogel. Still, modulation of the hydrogel properties by varying the amount of dispersed carbon nanotubes is challenging.

In this study, we present a new method for the preparation of supramolecular hybrid polymer-G4-based hydrogels by involving dextran (Dex) as the scaffolding soft polymer, controllably decorated with various amounts of guanosine utilizing benzene-1,4-diboronic acid (BDBA) as a linker (Fig. 1). The presented platform was developed as a tunable support with the precise control of the hydrogel internal structure and properties for cell growth applications. $K^+$ cations trigger the gelation process through G4 self-assembly and subsequent stacking, while the amount of guanosine units attached to Dex strongly influences the hydrogel properties and cell viability. Our reason for the tuning of gel properties is the presence of multiple 1,2-diols of the Dex sequence available for the condensation with guanosine mono-substituted benzene-1,4-diboronic acid through the formation of dynamic covalent cyclic boronate esters.[17] Recently, Wang and co-workers have reported random grafting of polyvinyl alcohol with guanosine using a boric acid linker.[18] Variations in the amounts of guanosine within the polyvinyl alcohol matrix led to considerable alterations in the gel's ionic conductivity and self-healing capability. As far as we know, there are no other reports on the use of the hybrid polymer-G4 strategy to prepare tunable soft hydrogel materials for biomedical applications.

We rationalized that Dex ($M_w$ = *ca.* 40 000) scaffolds could be controllably modified by various ratios of guanosine, which could self-assemble either intra- or intermolecularly in the presence of $K^+$. As illustrated in Fig. 1, we first reacted guanosine (G) and BDBA, in the presence of LiOH in water at 90 °C in a molar ratio of 1 : 1 : 2 corresponding to G/BDBA/LiOH. The formation of boronic ester between G and BDBA yielded a transparent solution after heating. Subsequently, three different quantities of G-BDBA solution were reacted with the same amount of Dex relating to the ratio of the Dex, available 1,2-diols and the amount of G-substituted boronate in the reaction. Addition of KCl resulted in the spontaneous formation of strong transparent hydrogels reminiscent to $K^+$ templated G-quartet assembly. We previously noted that the gelation process is very fast with the $K^+$, providing stronger hydrogels when compared

[a] "Petru Poni" Institute of Macromolecular Chemistry, Romanian Academy, Centre of Advanced Research in Bionanoconjugates and Biopolymers, Grigore Ghica Voda Alley 41 A, 700487, Iasi, Romania. E-mail: rotaru.alexandru@icmpp.ro
[b] "Petru Poni" Institute of Macromolecular Chemistry, Romanian Academy, Natural Polymers, Bioactive and Biocompatible Materials, Grigore Ghica Voda Alley 41 A, 700487, Iasi, Romania
[c] Institut Europeen Membranes, Adaptive Supramolecular Nanosystems Group, Université de Montpellier, ENSCM, CNRS, Pl Eugene Bataillon, CC47, F-34095, Montpellier 5, France. E-mail: mihail-dumitru.barboiu@umontpellier.fr

† Electronic supplementary information (ESI) available. See DOI: https://doi.org/10.1039/d2cc06881h

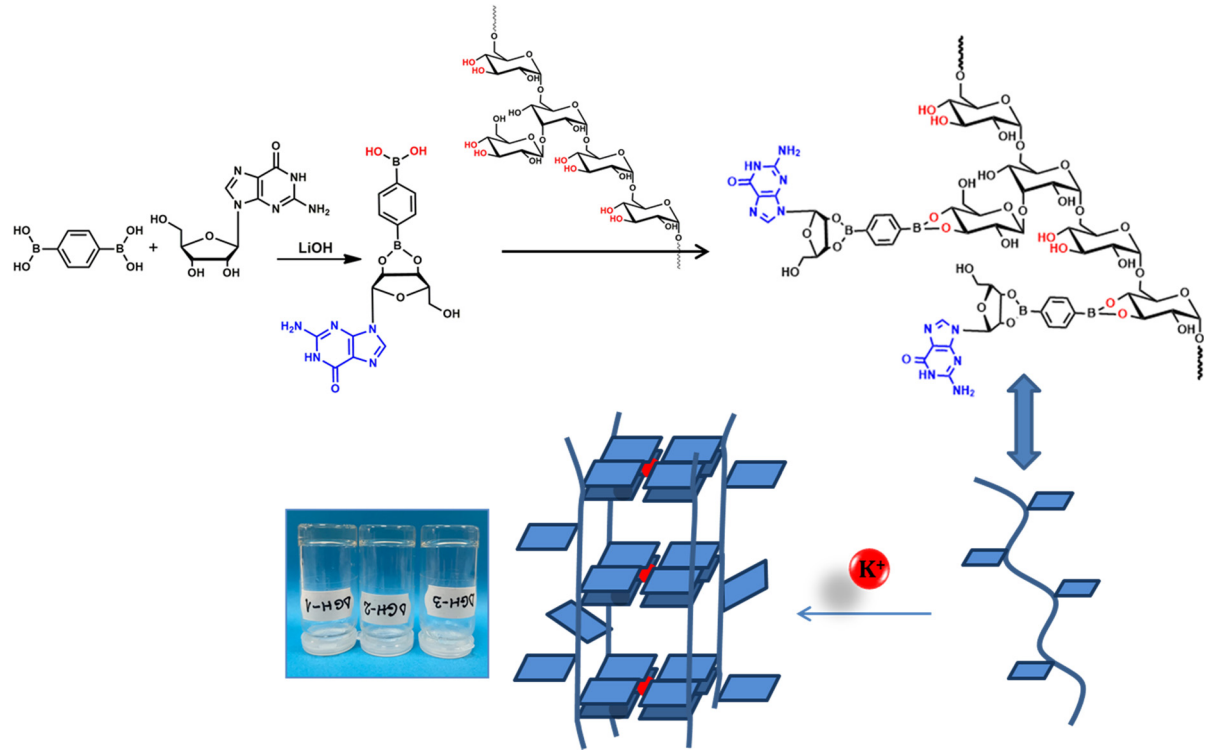


Fig. 1 Illustration of the dextran decoration with the guanosine mono-substituted benzene-1,4-diboronic acid moieties and subsequent self-assembly in the presence of $K^+$ into DGH hydrogels. Inset shows the prepared self-standing DGH1–3 hydrogels at 2 mL volume.

to other metal ions, $Ba^{2+}$, $Mn^{2+}$, $Fe^{3+}$ and $Ca^{2+}$.[8] The structures of hydrogels containing Dex decorated with 100% G (DGH1), 50% G (DGH2) and 30% G (DGH3) were confirmed by circular dichroism (CD), FTIR, and X-ray diffraction (XRD) analyses. The CD spectra of all hydrogels exhibited two major peaks, positive at 235 nm and 300 nm and a characteristic negative contribution at 260 nm, which correlates to the distinctive peaks of the G4-stacked structures (Fig. S1, ESI†).[11,19,20] In FTIR, the DGH1-3 xerogels compared to G and BDBA displayed characteristic changes for the formation of new bonds at 1800–1600 $cm^{-1}$ and 1400–1000 $cm^{-1}$ (Fig. S2, ESI†).[21,22]

The powder XRD diffractograms of the DGH1-3 xerogels further confirmed the formation of G4 stacks, revealing one broad diffraction peak at $d$ = 27.2° corresponding to the intermolecular $d$-spacing 3.3Å, a standard peak for the π–π distance between G-quartet stacks (Fig. S3, ESI†).[10,11] The amount of cross-linked G4 in each hydrogel induced changes in the internal structure as shown by the scanning electron microscopy (SEM) and atomic force microscopy (AFM) analyses of the xerogels (Fig. 2 and Fig. S4, ESI†). In SEM (Fig. 2a–c), all the lyophilized samples presented porous fibrillar morphologies, most probably formed of cross-linked columnar arrays of G4 on Dex interfaces. Interestingly, the higher cross-linking ratio gave less ordered morphology for the internal structure of DGH1 (Fig. 2a) when compared to that of DGH3 (Fig. 2c). We speculate that multiple G4 cross-linking points may induce random bending of the Dex scaffolds, while with the decrease of the cross-linking, the internal structure is more governed by the polymer template rather than only by the G4

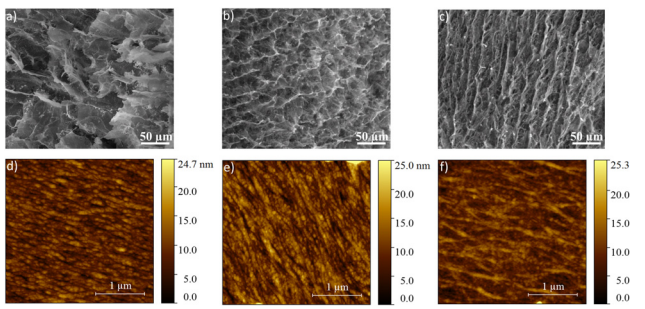


Fig. 2 SEM images of the (a) GDH1, (b) GDH2 and (c) GDH3 hydrogels (scale bar – 50 μm); AFM images of the (d) GDH1, (e) GDH2 and (f) GDH3 hydrogels (scale bar: 1 μm).

assembly and stacking, thus evidencing the more fibrillary nature of the morphology. The AFM images confirmed the fibrillar morphology of the DGH1-3 samples (Fig. 2d–f), revealing similar parallel alignments. The cross-section analysis (Fig. S4, ESI†) showed differences in the width of the fibrils depending on the G4 cross-linking degree of the Dex. DGH1 (Fig. 2d and Fig. S4a, ESI†) and DGH2 (Fig. 2e and Fig. S4b, ESI†) formed densely packed fibrils with different calculated mean width values (70 nm for DGH1 and 44 nm for DGH2). DGH3 on the other hand, presented the largest fibril width (87 nm, Fig. S4c, ESI†), but with less fibril density according to the cross-section.

All the investigated samples exhibited solid-like behaviour during the viscoelastic property investigations with values of

$G' > G''$ (Fig. S5a, ESI†). By increasing the G4 crosslinking degree from 30% of guanosine (DGH3) to 100% (DGH1), the $G'$ and $G''$ values increased by three and two orders of magnitude, respectively. The linear viscoelastic range (LVR) for each sample was identified in the shear stress ($\tau$) dependence of the viscoelastic moduli as being the domain where $G'$ and $G''$ are independent of the applied stress (Fig. S5b and Table S1, ESI†). After reaching a limit value of $\tau$ (yield point $\tau_y$), some micro breaks in the hydrogel network structure occur. $\tau_y$ represents the limit of LVR, and $G'$ remains still greater than $G''$ up to a critical value of $\tau$ (flow point $\tau_f$), from which the samples acquire liquid-like properties ($G' < G''$) due to the macro breaks in the network structure. The differences in the G4 crosslinking degree resulted in variations of the water retention capacity (Fig. 3, left). Vial inversion tests showed that DGH3 (30% of G) already collapsed at a volume of 3 mL and DGH2 (50% of G) collapsed at 4 mL. Meanwhile, DGH1 could bear up to 5 mL without collapsing. To estimate the structure recovery degree after deformation, oscillation–rotation–oscillation (O–R–O) tests were performed (Table S1 and Fig. S6, ESI†). DGH1 and DGH2 completely recovered their structure after 60 s from the interruption of the strong shear. In contrast, DGH3 did not recover its initial structure even until the end of the test, showing only a final structural recovery of 42%. These results evidence the thixotropic properties only for more crosslinked DGH1 and DGH2. The thixotropic behaviors of DGH1 and DGH2 were also visualized by vial inversion tests (Fig. 3, right); 2 mL self-standing samples (Fig. 3a) were mechanically shaken until becoming liquid (Fig. 3b), followed by 10 min relaxation to reform a firm hydrogel structure without collapsing (Fig. 3c).

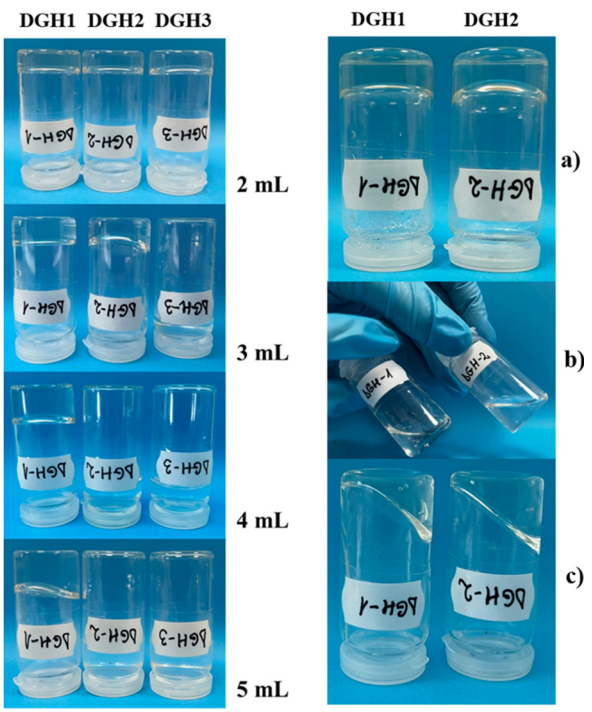


Fig. 3 Images of inversion vial tests for DGH1–3 in total volumes of 2–5 mL (left); thixotropic behavior (right) of DGH1 and DGH2 at 2 mL volume before (a) and after applying mechanical shaking (b), and after leaving the mechanically deformed hydrogels static for 10 min (c).

For potential applicability of DGH hydrogels for tissue engineering purposes, cell viability and growth tests on hydrogel supports on the NHDF (normal human dermal fibroblasts) cell line using all three hydrogels at a 2 mL volume were performed (Fig. 4). No washing or pH adjusting procedures as previously reported[10] were involved in sample preparation, the samples were utilized directly after preparation, and all three hydrogels exhibited great mechanical stability under the experimental conditions.

Colorimetric MTS cell proliferation assay[23] viability data illustrated the effect of the amount of G4 crosslinking in the DGH gels on cell growth (Fig. 4a). For all three samples incubated in the medium for 48 hours, a clear dependence of viability, calculated as a percentage relative to the viability of the control sample, on the amount of G attached to the Dex scaffold was noted. The results showed that DGH1 with the highest amount of G, benzene-1,4-diboronic acid and LiOH displayed the lowest cell viability values (35%) due to relatively high $Li^+$ concentrations[24] and elevated density of anionic diboronic esters, which in similar systems,[10] showed comparable cytotoxicity already after 24 hours of incubation. By contrast, cell viability was considerably enhanced to 83% for DGH2 and correspondingly to 96% for DGH3 as the result of lower amounts of grafted G-BDBA units and shielding of charged boronic esters by the non-toxic and biocompatible Dex protecting scaffold and using subsequent washing to remove the excess of $Li^+$ cations.[25,26] The observed cell viability data correlate with those of the previously reported systems containing $Li^+$, benzene-1,4-diboronic acid and G at similar concentrations.[16] The KCl utilized in all DGH samples should not alter the cell viability values due to the relatively low amounts (up to 90 mM), compared to the reported $K^+$ extracellular concentrations in *in vitro* investigations.[27]

The fluorescence microscopy images performed after 48 hours of incubation presented the NHDF cells' successful adherence to all three investigated sample surfaces, with cells actively migrating within the hydrogel volume and creating extended cellular projections, particularly observed on DGH1 and DGH2 (Fig. 4b–d). Unique hybrid polymer-G4 hydrogels with a tunable amount of G units were designed and prepared using dextran as the scaffolding template, benzene-1,4-diboronic acid as a dynamic covalent linker, and guanosine as a G4 former component. $K^+$ served as the templating cation during the self-assembly process, instantly yielding hydrogels with physical properties strongly depending on the amount of G units attached to the dextran template. CD and XRD techniques confirmed the formation of G-quartet structures within the hydrogel materials. The amount of G-quartet units within the hydrogel structures strongly influenced the rheological properties of the materials and their final biocompatibility. It was possible to tune the amount of G4 crosslinking moieties from 100% guanosine content (GDH1) to 50% (GDH2) without strongly altering the hydrogel properties, but considerably increasing its biocompatibility. Even at 30% guanosine content, the hydrogel maintained its high cell viability and

 

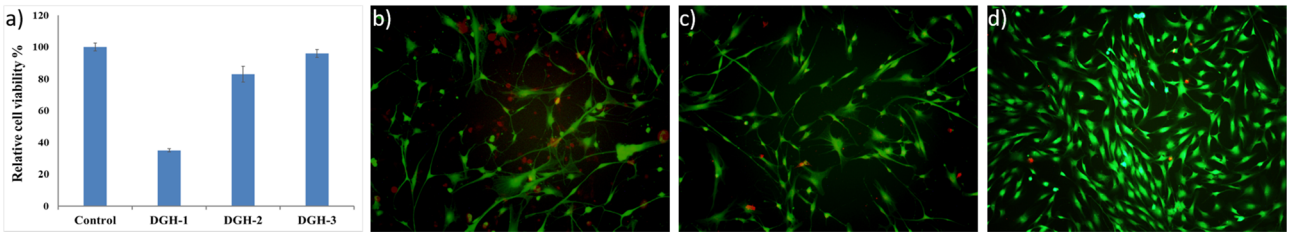


Fig. 4 (a) Cell viability (MTS assay) data compared with the control sample representing untreated NHDF cells supported by the culture medium (100%); microscopy images of the Live/Dead assay of NHDF cells on: (b) DGH1, (c) DGH2 and (d) DGH3 visualized after 48 h; live cells (green), dead cells (red).



strength to serve as a cell support. The performed 48 hours NHDF cell experiments indicated successful attachment and proliferation of cells into the hydrogel matrix creating extended cellular projections in all of the investigated samples.

This work presents a novel methodology in producing hydrogel materials,[28,29] bridging the dynamic polymeric and G4 supramolecular chemistry approaches, thus creating a tool for the preparation of tunable biocompatible hydrogels with thixotropic properties for potential applications in 3D bioprinting or regenerative medicine.

## Conflicts of interest

There are no conflicts to declare.

## Notes and references

1 Q. Tang, T. N. Plank, T. Zhu, H. Yu, Z. Ge, Q. Li, L. Li, J. T. Davis and H. Pei, *ACS Appl. Mater. Interfaces*, 2019, **11**, 19743–19750.
2 Z. Zhang, T. He, M. Yuan, R. Shen, L. Deng, L. Yi, Z. Sun and Y. Zhang, *Chem. Commun.*, 2015, **51**, 15862–15865.
3 J. Mayr, C. Saldías and D. D. Díaz, *Chem. Soc. Rev.*, 2018, **47**, 1484–1515.
4 G. M. Peters and J. T. Davis, *Chem. Soc. Rev.*, 2016, **45**, 3188–3206.
5 J. T. Davis, *Angew. Chem., Int. Ed.*, 2004, **43**, 668–698.
6 L. Stefan and D. Monchaud, *Nat. Rev. Chem.*, 2019, **3**, 650–668.
7 T. Bhattacharyya, P. Saha and J. Dash, *ACS Omega*, 2018, **3**, 2230–2241.
8 M. Godoy-Gallardo, M. Merino-Gómez, L. C. Matiz, M. A. Mateos-Timoneda, F. J. Gil and R. A. Perez, *ACS Biomater. Sci. Eng.*, 2023, **9**, 40–61.
9 A. Biswas, S. Maiti, D. M. Kalaskar and A. K. Das, *Chem. – Asian J.*, 2018, **13**, 3928–3934.
10 A. Rotaru, G. Pricope, T. N. Plank, L. Clima, E. L. Ursu, M. Pinteala, J. T. Davis and M. Barboiu, *Chem. Commun.*, 2017, **53**, 12668–12671.
11 M.-C. Sardaru, I. Rosca, S. Morariu, E.-L. Ursu, R. Ghiarasim and A. Rotaru, *Int. J. Mol. Sci.*, 2021, **22**, 9179.
12 J. Li, H. Wei, Y. Peng, L. Geng, L. Zhu, X.-Y. Cao, C.-S. Liu and H. Pang, *Chem. Commun.*, 2019, **55**, 7922–7925.
13 H. Wang, X.-Q. Xie, Y. Peng, J. Li and C.-S. Liu, *J. Colloid Interface Sci.*, 2021, **590**, 103–113.
14 S. Xiao, P. J. Paukstelis, R. D. Ash, P. Y. Zavalij and J. T. Davis, *Angew. Chem., Int. Ed.*, 2019, **58**, 18434–18437.
15 T. Jungst, W. Smolan, K. Schacht, T. Scheibel and J. Groll, *Chem. Rev.*, 2016, **116**, 1496–1539.
16 E.-L. Ursu, G. Gavril, S. Morariu, M. Pinteala, M. Barboiu and A. Rotaru, *Mater. Sci. Eng., C*, 2020, **111**, 110800.
17 T. Figueiredo, V. Cosenza, Y. Ogawa, I. Jeacomine, A. Vallet, S. Ortega, R. Michel, J. D. M. Olsson, T. Gerfaud, J.-G. Boiteau, J. Jing, C. Harris and R. Auzély-Velty, *Soft Matter*, 2020, **16**, 3628–3641.
18 K.-P. Wang, Y. Yang, Q. Zhang, Z. Xiao, L. Zong, T. Ichitsubo and L. Wang, *Mater. Chem. Front.*, 2021, **5**, 5106–5114.
19 G. M. Peters, L. P. Skala, T. N. Plank, B. J. Hyman, G. N. Manjunatha Reddy, A. Marsh, S. P. Brown and J. T. Davis, *J. Am. Chem. Soc.*, 2014, **136**, 12596–12599.
20 A. Biswas, S. Malferrari, D. M. Kalaskar and A. K. Das, *Chem. Commun.*, 2018, **54**, 1778–1781.
21 Y. Li, Y. Liu, R. Ma, Y. Xu, Y. Zhang, B. Li, Y. An and L. Shi, *ACS Appl. Mater. Interfaces*, 2017, **9**, 13056–13067.
22 C. Arnal-Hérault, A. Pasc, M. Michau, D. Cot, E. Petit and M. Barboiu, *Angew. Chem., Int. Ed.*, 2007, **46**, 8409–8413.
23 J. C. Stockert, A. Blázquez-Castro, M. Cañete, R. W. Horobin and A. Villanueva, *Acta Histochem.*, 2012, **114**, 785–796.
24 M. S. Allagui, C. Vincent, A. El feki, Y. Gaubin and F. Croute, *Biochim. Biophys. Acta, Mol. Cell Res.*, 2007, **1773**, 1107–1115.
25 S.-H. Hyon, N. Nakajima, H. Sugai and K. Matsumura, *J. Biomed. Mater. Res., Part A*, 2014, **102**, 2511–2520.
26 C. Wang, J. You, M. Gao, P. Zhang, G. Xu and H. Dou, *Nanomedicine*, 2020, **15**, 1285–1296.
27 E. M. Garland, J. M. Parr, D. S. Williamson and S. M. Cohen, *Toxicol. In Vitro*, 1989, **3**, 201–205.
28 S. Xiao, W. Lee, F. Chen, P. Y. Zavalij, O. Gutierrez and J. T. Davis, *Chem. Commun.*, 2020, **56**, 6981–6984.
29 Y. Du, T. Liu, F. Tang, X. Jin, H. Zhao, J. Liu, X. Zeng and Q. Chen, *Chem. Commun.*, 2021, **57**, 12936–12939.